E-ISSN 2586-9027
Homepage : https://tci-thaijo.org/index.php/SciTechAsia Science & Technology Asia
Vol. 30 No.1 January - March 2025 Page: [70-78]
Original research article

Hydroxyapatite/MgO Composites from Biowaste Pokea Clam Shells (Batissa violacea): Structure and Mechanical Properties for Medical Application

Armid, Fahmiati, Halimahhtussaddiyah Ritonga, Muh. Nurhidayat, Laode A. Kadir*

Department of Chemistry, Halu Oleo University, Southeast Sulawesi 93232, Indonesia

Received 18 September 2024; Received in revised form 27 February 2025
Accepted 14 March 2025; Available online 24 March 2025

ABSTRACT

In this research, hydroxyapatite was prepared from Pokea clam shells as home industrial waste by a hydrothermal method. HAp-MgO composites were successfully synthesized through an in-situ hydrothermal technique. The impact of MgO incorporation on the mechanical characteristics of HAp and its composites with 5 wt.% MgO was investigated. An X-ray diffraction (XRD) was used for samples characterization and to assess their phase stabilities. The existence of MgO in the composite material was indicated by its specific peaks at 37.6° and 26.7°. Several indices, including both hardness and compressive strength, were used to measure the mechanical characteristics of genuine HAp and HAp-MgO composite. We found that the inclusion of MgO considerably improved HAp's mechanical characteristics and particle growth. The best mechanical properties were observed in the HAp-MgO composite sintered at 900ºC with 5 wt.% MgO. This composite exhibited a hardness of 30.72 VHN and a compressive strength of 3.12 MPa. The present study recommends that composites with mechanical properties are suitable for biomedical purposes.

Keywords: Hydroxyapatite; HAp-MgO composite; Hydrothermal; Pokea clam shells; Mechanical properties

1. Introduction

For many years, research has been conducted on bone-emulating biomaterials to attain high mechanical strength without affecting other qualities. However, the problem of creating a bone substitute material that is as strong as natural bone has remained largely unsolved. Several metallic implants, such as those made of MgO alloys, MgO-Aluminium alloys, have been used as bone

***Corresponding author:** laode.kadir90@uho.ac.id **doi:** 10.14456/scitechasia.2025.5

substitutes and exhibit basically neuter performance when applied as permanent fixtures in vivo [1, 2]. Metallic implantations are avoided because of the restriction on the production of harmful metallic ions, notwithstanding their greater strength potential when compared to natural bone. Additionally, the stress shielding effect is caused by mechanical qualities that are not compatible with natural tissues, such as density and biocompatibility [3]. Various methods might be used to fabricate bone materials with managed physicochemical properties [4]. The establishment of such biomaterials with mechanical strength is appreciably comparable to that of natural bone and a great in vivo response. Because of the long-distance linked channels that allow cell development and curing to create these biomaterials site active, they are capable of hard tissue restoration and reconstruction. Bio ceramic materials have distinctive physical characteristics and biological reactions to cell adhesion and migration [5]. Bio ceramic, also known as bio ceramic materials, can be bioactive (such as hydroxyapatite), bioinert (such as alumina and zirconia), or resorbable (such as tri-calcium phosphate). The most important components of living tissues are calcium phosphate minerals, which provide biological hard tissue (such as bones, teeth, and tendons) stability and strength [6]. Tricalcium phosphate (-TCP) and tetra tricalcium phosphate are the subsequent phases that result from the breakdown of HAp at higher temperatures (TTCP). At higher temperatures, they are the most noticeable stable phases; however, under physiologically normal settings, they are less stable and degradable [7]. Therefore, they cannot be used as weight-bearing implants. The creation of bone cement completely utilizes its degradative nature. Aside from being stable in vivo, HAp is also bioactive and encourages bone ingrowth after implantation [8].

In terms of chemical composition, hydroxyapatite [$Ca_{10}(PO_4)_6(OH)_2$] is identical to the inorganic compound of natural bones and teeth. The properties of HAp, including its surface morphology, structure, crystallinity, and interconnecting porous material resembling natural bones, determine its biological uses, biocompatibility, and bioactive characteristics. Nanostructured HAp powders are ideal biomaterials for bone grafts, bone filler substitutes, and implant materials as they are highly osteoconductive and biocompatible. Furthermore, HAp has a stable thermal dielectric, diamagnetic, and the capacity to induce bone development. All these characteristics suggest that it might be used in the biomedical business [9, 10]. The production of HAp from seashells has been attempted on several occasions. HAp production utilizes a variety of seashells as calcium precursors [11]. According to Rodriguez et al., the conversion of aragonite minerals to HAp was more effective than the conversion of the calcite phase of calcium carbonate to HAp [12]. HAp is made from calcium carbonate extracted from various shells, including garden snails, conchs, and enormous clams. In a previous study, di-ammonium phosphate ($(NH_4)_2HPO_4$) was employed with CaO as a source to synthesize HAp using a hydrothermal technique, whereby the FTIR analysis revealed a very pure and crystalline HAp powder [8].

Pure HAp has a limited range of applications for replacing missing bone because of its inferior mechanical strength compared with real bone and teeth [13]. No biomaterial capable of withstanding forces as large as human bone has yet been developed. The porosity and formation of secondary phases, among other microstructural features, have an impact on the strength and other mechanical properties of HAp. Owing to the pore interactions, the porosity of a biomaterial is crucial for tissue regeneration. Due to normal tissue growth and the absence of negative reactions, the porosity characteristics of HAp as a substitute bone-material provide mechanical support. The porous architecture and pore size have a significant impact on the mechanical characteristics of porous HAp

[14]. By substituting, doping, and/or including certain additives into its composites, hydroxyapatite can be customized for the desired mechanical strength and deterioration to replicate real bone [15]. Since pure HAp has very poor mechanical performance, several biocompatible compounds (metal oxides and carbonates) have been mixed with synthetic HAp to create a variety of composites with improved bioactivity and mechanical qualities without changing biological characteristics. An earlier study attempted to explore the mechanical properties of various biocompatible oxide additions, including silica (SiO_2), zirconia (ZrO_2), alumina (Al_2O_3), (r-GO), cerium oxide (CeO_2), and MnO_2 [16]. The densification and mechanical characteristics of the sintered HAp composites at low temperatures were observed to benefit more from a small amount of this additive. The mechanical and biodegradable features of MgO materials and alloys are particularly desirable for bone and dental applications owing to their high biocompatibility, excellent degradability, lower weight, and good density [17]. Since the rapid regeneration of the host material is caused by the slow release of Mg ions from the implanted materials, MgO-containing HAp is frequently employed as a bone graft material. MgO incorporation is anticipated to have a considerable impact on the grain development of HAp and enhance its mechanical properties [18, 19].

In the present study, a thorough investigation of the impact of the amounts of MgO 5 wt.% on the mechanical properties of HAp was conducted in sequence to identify the correct strength of HAp. First, using a hydrothermal process, pure HAp powder was created. This method is well-known for producing high-crystalline HAp powder. Additionally, an approximated amount of MgO was added to HAp to create the MgO-HAp composites. Using several methods, including SEM and XRD, the surface and structural characteristics of HAp and HAp/MgO samples were studied. The most reliable testing (Universal Testing Machine (UTM) Instron 5944) was also performed to examine the mechanical characteristics of prepared HAp and its composites.

2. Materials and Methods

2.1 Materials and method for synthesis

Diammonium dihydrogen phosphate ($(NH_4)_2HPO_4$) and MgO (>99% Merck) were used as starting materials in the manufacture of HAp powder. The calcium source was recovered from biowaste Pokea clam shells, collected from Pohara River, Southeast Sulawesi, Indonesia. No additional purification was performed prior to using any compound. Biowaste Pokea clam shells were cleaned properly and washed to remove any contaminants. The shell was then dried, put into an electrical furnace, and heated at a temperature of 900°C for 4 hours for calcination process. The calcium carbonate ($CaCO_3$) in the Pokea clam shell was converted to calcium oxide (CaO) during the calcination process by releasing carbon dioxide (CO_2) [20, 21].

A variety of methods are available for the synthesis of hydroxyapatite, including sol-gel processes, hydrothermal techniques, precipitation reactions in a wet chemical environment, and solid-state and mechanochemical reactions in a dry framework [22, 23]. HAp synthesis was carried out by mixing 14 grams of calcium oxide (CaO) from Pokea clam shells with 17.25 grams of diammonium hydrogen phosphate $(NH_4)_2HPO_4$ at a substrate mole ratio of 1.67. The mixed compound was put into a hydrothermal autoclave and heated in an oven at a temperature of 200°C for 72 hours. The resultant solid material was washed with distilled water until reaching neutral pH. Subsequently, it was heated at 110°C temperature for 24 hours, followed by sintering at a temperature of 900°C for 5 hours [24].

In-situ synthesis of the hydroxyapatite composite was carried out by mixing calcium oxide (CaO) from Pokea shells with ammonium dihydrogen phosphate

$(NH_4)H_2PO_4$, then adding 5% weight of MgO. The mixture was put into a hydrothermal autoclave and heated in an oven at 200°C temperature for 72 hours. The resultant solid material was washed with distilled water until reaching neutral pH before being heated 110°C for 24 hours, followed by sintering at 900°C for 5 hours [15].

2.2 Materials characterizations

The elemental composition of Pokea clam shell composition was measured using X-ray fluorescence (XRF, Rigaku Nex CG). A Rigaku Minifex-II X-ray diffractometer outfitted with monochromatic Cu-Kα radiation (λ = 0.15418 nm) was used to record the XRD patterns. The Crystallography Open Database (COD ID number: 2300273 was used to compare the pure HAp and sintered HAp/MgO composites (standard data for hexagonal HAp). Using an FTIR spectrometer with a range of 4000-500 cm^{-1}, the intra/intermolecular interactions between MgO-HAp were investigated (ATR FT-IR spectrometer).

A Scanning Electron Microscope (SEM) EVOMA10 was utilized to examine the composite morphology and microstructures of fractures in HAp and HAp/MgO composites. Utilizing a mechanical testing machine (UTM Instron 5944) in compression mode on cylindrical pellets with dimensions of 1.3 cm in diameter and 2.0 cm in length/height, the mechanical characteristics of HAp/MgO composite samples were evaluated by employing a mechanical testing machine (UTM Instron 5944). The temperature was applied at 28°C during characterization.

3. Results and Discussion

3.1 CaO content of Pokea clam shell

The calcium oxide (CaO) content of Pokea clam shell revealed from this study was 98.43%. This indicates that the $CaCO_3$ from Pokea clam shells have been successfully converted into CaO. This result is not significantly different from the results gained by Desmond [7] who obtained CaO from mussel and scallop shell yields of 98.36% and 97.53%, respectively. Table 1 shows the mineral composition of Pokea clam shell in the oxide form after calcination analysed by XRF.

Table 1. Composition of Pokea clam shell from XRF analysis.

Minerals	Content (%)		
	Mussel Shell [7]	**Scallop Shell** [12]	**Pokea Clam Shell** [this work]
CaO	98.36	97.52	98.43
Na_2O	0.93	0.56	0.24
Al_2O_3	0.29	1.56	0.62
Fe_2O_3	0.16	0.24	0.02
MgO	0.15	0.10	0.06
Balance	0.11	0.02	0.63

3.2 Composite XRD Analysis

The XRD diffractograms of the synthetic HAp and HAp/MgO with 5 wt.% of MgO are shown in Fig. 1. The production of pure and crystalline HAp samples was indicated by the appearance of strong and very high intensity XRD diffractogram, which corresponded to the COD file (ID number 2300273). No secondary phases or other contaminants were observed in the XRD diffractogram of pure HAp sample. Except for minor MgO peaks, the XRD pattern of the HAp/MgO composite was basically identical to that of pure HAp. Since Mg was substituted into HAp, the development of the typical MgO peak at 37.6° and 26.7° indicated the presence of MgO [26].

Table 2. Lattice parameters.

Sample	D (nm)	a=b (Å)	c (Å)	α=β (°)	γ (°)
HAp*		9.424	6.879	90	120
HAp synthesis	46.15	9.448	6.921	90	120
HAp-MgO synthesis	31.72	9.501	7.104	90	120

HAp* points out the standard data belonging to the COD ID 9011096

Calculation of the HAp crystal size gave an average of 46.15 nm compared to 31.72 nm for HAp-MgO. The details of the calculation result can be seen in Table 2. The result obtained in this study is not significantly

different from the results previously reported by Mohammed [27] and Korkmas [28]. The calculation yielded a degree of crystallinity of 85.43% for HAp, and 93.11% for HAp-MgO. These results indicate that the addition of MgO to the composite enhances its crystallite properties.

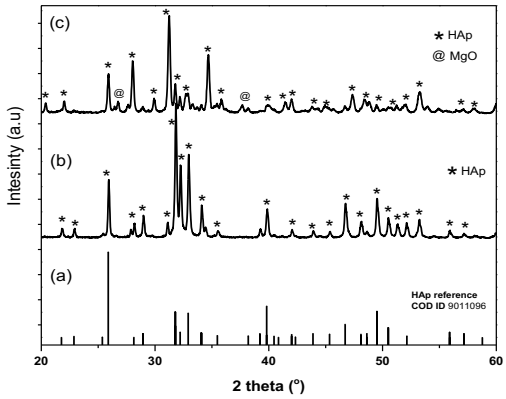

Fig. 1. XRD of HAp and MgO–HAp composites in scanning range 20–60° (a) HAp reference, (b) HAp experiment, (c) HAp-MgO composite experiment.

3.3 Composite FTIR Analysis

To examine the chemical structure of the manufactured samples, FTIR analysis of the samples was also performed. The transmittance spectra of pure HAp and HAp/MgO composite are shown in Fig. 2. The OH- stretching and the less intense calcite-specific peaks produced an intense peak at 3572 cm^{-1}, as seen in typical stretching. The hydroxyl (OH-) group is responsible for the medium peaks at 634 cm^{-1} and 3572 cm^{-1} (stretching vibration) [17]. The high transmittance bands between 926 and 1084 cm^{-1} are the usual stretching bands of O-P-O in PO_4^{-3} of HAp. A similar observation has been reported in the literature [18]. This band also shifted blue to 971 cm^{-1} when MgO was added, which might be due to the asymmetric binding mode of O-P in PO_4^{-3}. A weak transmittance spectrum observed at 598 cm^{-1} was due to a symmetric binding mode of O-P in PO_4^{-3}. In line with the study results of Yanovska et al. [19], the existence of carbonate content in HAp can be explained by the presence of CO_3^{2-} bands observed at wavenumbers between 1565 and 1815 cm^{-1} (v_3). The similar observation was made in this occurrence (Fig. 2), and the carbonate content of the composite was revealed.

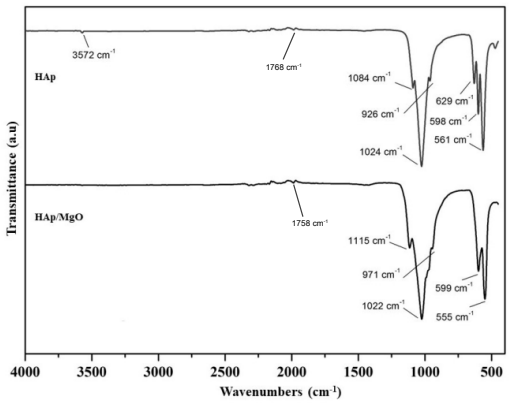

Fig. 2. FTIR Analysis of composite in range of 500–4000 cm^{-1} sintered at 900°C (a) synthetic HAp, (b) HAp-MgO composite.

3.4 Mechanical behaviour

The compressive strength and hardness of hydroxyapatite HAp depending on the porosity and composition of the material. Fig. 3 shows mechanical behaviours of HAp and MgO–HAp composite. The compressive strength and hardness of HAp are 1.8 MPa and 20.33 VHN. These values were lower than previous reported by Kareem [29] .The compressive strength value increases drastically to be 3.12 MPa with the addition of MgO (Fig. 3(b)). This result is in accordance with the findings of [20] which found that the use of MgO can increase inter-particle densification. In addition, particle unification and compaction are facilitated by the high temperature thermal process, hence the bonds between the grains are strengthened. The compaction process improves the mechanical characteristics.

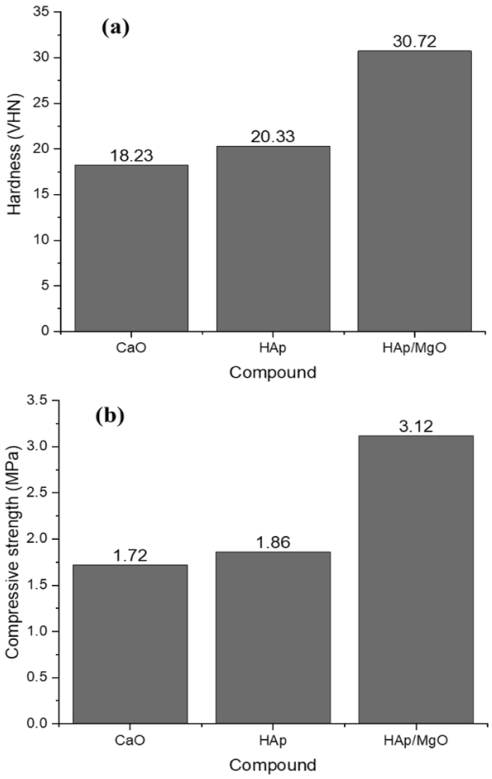

Fig. 3. Mechanical behaviors of HAp and MgO–HAp composite samples at sintering temperature of 900ºC, (a) Hardness (b) Compressive strength.

Based on the results of the hardness analysis illustrated in Fig. 3, CaO has a hardness value of 18.23 VHN, while HAp has a value of 20.33 VHN and the HAp-MgO composite is 30.72 VHN. This study supports the observations [30] which found that the hardness value increases with increases to the compressive strength. Accordingly, the material become denser and tougher. This is caused by increased pressure on the inter-grain connection, so that the distance between the grains become closer and the space between the grains become smaller.

3.5 Morphological properties

Fig. 4 shows the surface morphologies of the HAp and HAp-MgO cracked samples sintered at 900ºC. It is clear from the images that the addition of MgO has a significant effect on the development of HAp grain, leading to an increase in mechanical characteristics. The microstructure of HAp-MgO composite shows proper grain development. The pores are marked with bright white circles [31], [32]. The SEM image of the pure HAp sample (Fig. 4(a)) shows the presence of various pores with irregular shape, some of which are related to one another. Therefore, the pure HAp sample has poorer porosity, low composition and other mechanical properties compared to its composite. Despite MgO being highly fusible into linked pores to reduce porosity, a relatively denser microstructure is produced because of its inclusion [33]. At 900ºC, it was anticipated that the MgO articles would melt and aid in the densification of the HAp sample. The composite shown in Fig. 4(b) with 5 wt.% MgO shows the best porous morphology. Most of the pores in the HAp grains are located at their grain borders. Pores that are comparatively regular and homogeneous can be observed in the HAp-MgO composite (Fig. 4(b)). In addition, synthetic HAp exhibits a highly porous structure and the pores are unevenly distributed throughout the image.

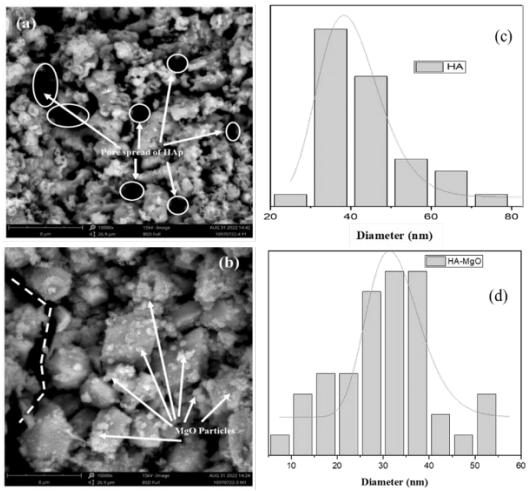

Fig. 4. SEM images of synthetic HAp and HAp/MgO composite (a) HAp (b) HAp-MgO composite (c) HAp diameter distribution (d) HAp-MgO diameter distribution.

4. Conclusion

In this study, pure HAp and HAp-MgO composites were successfully prepared by a hydrothermal method. The addition of MgO to pure HAp and the sintering temperature were determined based on the hardness and compressive strength of several mechanical parameters. The present study found that the HAp-MgO composite was very beneficial for densification to achieve the highest density, hardness, and compressive strength. It is noted that the porosity has a significant impact on the mechanical characteristics and degradability.

Acknowledgements

We acknowledge the financial support from the Ministry of Education, Culture, Research and Technology of the Republic of Indonesia. The authors thanks to Department of Chemistry Laboratory, University of Halu Oleo, Kendari, Indonesia, for providing all resources for performing the research and LPPMP Halu Oleo University for their administration support

References

[1] He M, Chen L, Yin M, Xu S, Liang Z. Review on magnesium and magnesium-based alloys as biomaterials for bone immobilization. Journal of Materials Research and Technology. 2023;23:4396–419.

[2] Obaıd Kareem R, et al. Exploring the Influence of Various Solvents on the Structural, Optical, and Spectroscopic Properties of MgO. El-Cezeri Fen ve Mühendislik Dergisi, May 2024.

[3] George SM, Nayak C, Singh I, Balani K. Multifunctional Hydroxyapatite Composites for Orthopedic Applications: A Review. ACS Biomater Sci Eng, Aug. 2022;8(8):3162–86.

[4] George SM, Nayak C, Singh I, Balani K. Multifunctional Hydroxyapatite Composites for Orthopedic Applications: A Review. ACS Biomater Sci Eng. Aug. 2022; 8(8); 3162–86.

[5] Tosan F, Fathi AH, Yari A, Rahnama N, Sakhaei D. Effects of doping metal nanoparticles in hydroxyapatite in Improving the physical and chemical properties of dental implants. Nanomedicine Research Journal. Nov. 2021; 6(4); 327–36.

[6] Fu Z, Cui J, Zhao B, Shen SG, Lin K. An overview of polyester/hydroxyapatite composites for bone tissue repairing. J Orthop Translat. May 2021;28:118–30.

[7] Amin A, Ulfah M. Sintesis Dan Karakterisasi Komposit Hidroksiapatit Dari Tulang Ikan Lamuru (Sardilnella Longiceps)-Kitosan Sebagai Bone Filler. Jurnal Farmasi UIN Alauddin Makassar, Apr. 2017;5(1):9–15.

[8] Sukmana I, Eka Risano AY, Arif Wicaksono M, Adi Saputra R. Perkembangan dan Aplikasi Biomaterial dalam Bidang Kedokteran Modern: A Review. Insologi: Jurnal Sains dan Teknologi. Oct. 2022;1(5):635–46.

[9] Kareem RO, Bulut N, Kaygili O. Hydroxyapatite Biomaterials: A Comprehensive Review of their Properties, Structures, Medical Applications, and Fabrication Methods. Journal of Chemical Reviews. Jan. 2024;6(1):1–26,

[10] Kareem RO, et al. Experimental and theoretical characterization of Bi-based hydroxyapatites doped with Ce. Ceram Int. Nov. 2022;48(22):33440–54.

[11] Desmond S, Kurniawan D, Nor FM. Synthesis of hydroxyapatite from seashells via calcination at various temperature using microwave and furnace. AIP Conf Proc. Apr. 2020;2217;(1):020010.

[12] Rodríguez-Vázquez M, Ramos-Zúñiga R. Chitosan-Hydroxyapatite Scaffold for Tissue Engineering in Experimental Lumbar Laminectomy and Posterolateral Spinal Fusion in Wistar Rats. Asian Spine J. 2020;14(2).

[13] Ridi F, Meazzini I, Castroflorio B, Bonini M, Berti D, Baglioni P. Functional calcium phosphate composites in nanomedicine. Adv Colloid Interface Sci. Jun. 2017;244:281–95.

[14] Hartatiek, J, Utomo LI, Noerjannah NZ, Rohmah, Yudyanto. Physical and mechanical properties of hydroxyapatite/polyethylene glycol nanocomposites. Mater Today Proc. Jan. 2021;44:3263–7.

[15] Ingole VH, Ghule SS, Vuherer T, Kokol V, Ghule AV. Mechanical Properties of Differently Nanostructured and High-Pressure Compressed Hydroxyapatite-Based Materials for Bone Tissue Regeneration. Minerals 2021. Dec. 2021;11(12): 1390.

[16] Gautam CR, Kumar S, Biradar S, Jose S, Mishra VK. Synthesis and enhanced mechanical properties of MgO substituted hydroxyapatite: A bone substitute material. RSC Adv. 2016;6(72):67565–74.

[17] Fu Z, Cui J, Zhao B, Shen SG, Lin K. An overview of polyester/hydroxyapatite composites for bone tissue repairing. J Orthop Translat. May 2021;28:118–30.

[18] Mahmood BK, et al. Structural, magnetic, thermal, biocompatibility, and electronic properties of lanthanum doped-magnesium hydroxyapatite. Ceram Int, Feb. 2025.

[19] Bulut N, et al. Mg-Dopant Effects on Band Structures of Zn-Based Hydroxyapatites: A Theoretical Study. Iranian Journal of Science. Dec. 2023;47(5–6):1843–59.

[20] Alimuddin A, Agusriyadin A, Fahmiati F, Dicki Pratama Muh, Kadir LA. The Quality Study of Hydroxyapatite (HAp)-TiO2 Composites from Pokea (Batissa violacea var. celebensis) Shell Waste by Hydrothermal, Microwave and Precipitation Methods. Engineering And Technology Journal. Nov. 2024;9(11):5489–94.

[21] Agusriyadin, Fahmiati, Faradissa, Armid, Kadir LA. Studi Sitoksisitas dan Sifat Mekanik Nano Hidroksiapatit Dari Cangkang Kerang Pokea (Batissa violacea var. celebensis, von Martens 1897). BioWallacea: Jurnal Penelitian Biologi (Journal of Biological Research). Feb. 26, 2025;10(2):64–73.

[22] Mohammed BA, et al. The effects of pH on the morphology and structural properties of Er/Yb co-doped hydroxyapatite. Journal of Physical Chemistry and Functional Materials. Jun. 2024;7(1):11–6.

[23] Keser S, Dogan A, Ates T, Barzinjy AA, Ates B, Tekin S, Sandal S, Kareem RO, Özcan İ, Bulut N, Kaygili O. Effects of gallic acid and quercetin on the structural, thermal, spectroscopic, in vitro biocompatibility and electronic properties of Au-based hydroxyapatite structure. Mater Chem Phys. Nov. 2024;327:129892.

[24] Mohd Pu'ad NAS, Abdul Haq RH, Mohd Noh H, Abdullah HZ, Idris MI, Lee TC. Synthesis method of hydroxyapatite: A review. Mater Today Proc. Jan. 2020;29:233–9.

[25] Hutabarat GS, Qodir DT, Setiawan H, Akbar N, Noviyanti AR. Sintesis Komposit Hidroksiapatit-Lantanum Oksida (HA-La2O3) dengan Metode Hidrotermal secara In-Situ dan Ex-Situ. ALCHEMY Jurnal Penelitian Kimia. Sep. 2019;15(2):287.

[26] Catarina CC, Tatiana P, Laura C, Marta TP, Paulo CC, Valentina FD, Paulo AQ, Fernando JM, Susana RS. The antibacterial and angiogenic effect of magnesium oxide in a hydroxyapatite bone substitute. Scientific Reports 2020. Nov. 2020;10(1):1–15.

[27] Mohammed BA, Ateş T, Mahmood BK, Kareem RO, Keser S, Bulut N, Kaygılı O. Investigation of the effects of glycerol addition as a catalyst on the morphology and structural properties of Gd/Er co-doped hydroxyapatite. Journal of Physical Chemistry and Functional Materials. Jun. 2024;7(1):28–31.

[28] Korkmaz AA, Lana OA, Rebaz OK, Hanifi K, Tankut A, Niyazi B, Omer K, Burhan A. Theoretical and experimental characterization of Sn-based hydroxyapatites doped with Bi. Journal of the Australian Ceramic Society. Jul. 2022;58(3):803–15.

[29] Kareem RO, Kaygili O. Synthesis and Characterization of Bismuth-Based Hydroxyapatites Doped with Cerium. 2023.

[30] Le BT, Ramesh S, Long BD, Son NA, Munar M, Shi X. Effect of MgO addition on the sinterability, mechanical properties and biological cell activities of sintered silicon-substituted hydroxyapatite. Journal of the Australian Ceramic Society. Mar. 2021;57(3):857–68.

[31] Sopyan I, Pusparini E, Ramesh S, Tan CY, Ching YC, Wong YH, Zainal Abidin NI, Hari C, Ramesh S, Bang LT. Influence of sodium on the properties of sol-gel derived hydroxyapatite powder and porous scaffolds. Ceram. 2017;43:12263–9.

[32] Tawfik HQ, Ramesh S, Yusof F, Wan JB, Chin YC, Hari C, Ramesh S, Krishnasamy S. Micro-arc oxidation of bioceramic coatings containing eggshell-derived hydroxyapatite on titanium substrate. Ceram. 2019;45:18371–81.

[33] Pei F, Rongyang Z, Liuyimei Y, Shijie C, Dong W, Hao P, Cijun S. Hydrothermal synthesis of hydroxyapatite nanorods and their use in PCL bone scaffold. Ceram Int, Nov. 2022.